REGULAR ARTICLE

blood advances

A unifying hypothesis for PNMZL and PTFL: morphological variants with a common molecular profile

Julia Salmeron-Villalobos,[1,2,*] Caoimhe Egan,[3,*] Vanessa Borgmann,[4,*] Inga Müller,[4] Blanca Gonzalez-Farre,[1,2] Joan Enric Ramis-Zaldivar,[1,2] Dominik Nann,[4] Olga Balagué,[1,2] Mónica López-Guerra,[1,2] Dolors Colomer,[1,2] Ilske Oschlies,[5] Wolfram Klapper,[5] Selina Glaser,[6] Young Hyeh Ko,[7] Irina Bonzheim,[4] Reiner Siebert,[6] Falko Fend,[4] Stefania Pittaluga,[3] Elias Campo,[1,2] Itziar Salaverria,[1,2,†] Elaine S. Jaffe,[3,†] and Leticia Quintanilla-Martinez[4,8,†]

[1]Hematopathology Unit, Hospital Clínic of Barcelona, Institut d'Investigacions Biomèdiques August Pi i Sunyer (IDIBAPS), University of Barcelona, Barcelona, Spain; [2]Centro de Investigación Biomédica en Red de Cáncer (CIBERONC), Madrid, Spain; [3]Hematopathology Section, Laboratory of Pathology, National Cancer Institute, Bethesda, MD; [4]Institute of Pathology and Neuropathology, Eberhard Karls University of Tübingen and Comprehensive Cancer Center, University Hospital Tübingen, Tübingen, Germany; [5]Institute of Pathology, Hematopathology Section and Lymph Node Registry, Christian-Albrechts-University of Kiel, Kiel, Germany; [6]Institute of Human Genetics, Ulm University and Ulm University Medical Center, Ulm, Germany; [7]Department of Pathology, Samsung Medical Center, Seoul, South Korea; and [8]Cluster of Excellence iFIT, "Image-Guided and Functionally Instructed Tumor Therapy," University of Tübingen, Tübingen, Germany

Key Points

- PNMZL has a molecular landscape characterized by low genomic complexity and frequent *MAP2K1*, *TNFRSF14*, and *IRF8* alterations.
- The histologic and molecular features of PNMZL and PTFL suggest that they represent a morphologic spectrum of the same biologic entity.

Pediatric nodal marginal zone lymphoma (PNMZL) is an uncommon B-cell neoplasm affecting mainly male children and young adults. This indolent lymphoma has distinct characteristics that differ from those of conventional nodal marginal zone lymphoma (NMZL). Clinically, it exhibits overlapping features with pediatric-type follicular lymphoma (PTFL). To explore the differences between PNMZL and adult NMZL and its relationship to PTFL, a series of 45 PNMZL cases were characterized morphologically and genetically by using an integrated approach; this approach included whole-exome sequencing in a subset of cases, targeted next-generation sequencing, and copy number and DNA methylation arrays. Fourteen cases (31%) were diagnosed as PNMZL, and 31 cases (69%) showed overlapping histologic features between PNMZL and PTFL, including a minor component of residual serpiginous germinal centers reminiscent of PTFL and a dominant interfollicular B-cell component characteristic of PNMZL. All cases displayed low genomic complexity (1.2 alterations per case) with recurrent 1p36/*TNFRSF14* copy number–neutral loss of heterozygosity alterations and copy number loss (11%). Similar to PTFL, the most frequently mutated genes in PNMZL were *MAP2K1* (42%), *TNFRSF14* (36%), and *IRF8* (34%). DNA methylation analysis revealed no major differences between PTFL and PNMZL. Genetic alterations typically seen in conventional NMZL were absent in PNMZL. In summary, overlapping clinical, morphologic, and molecular findings (including low genetic complexity; recurrent alterations in *MAP2K1*, *TNFRSF14*, and *IRF8*; and similar methylation profiles) indicate that PNMZL and PTFL are likely part of a single disease with variation in the histologic spectrum. The term "pediatric-type follicular lymphoma with and without marginal zone differentiation" is suggested.

Submitted 15 February 2022; accepted 10 May 2022; prepublished online on *Blood Advances* First Edition 24 May 2022; final version published online 12 August 2022. DOI 10.1182/bloodadvances.2022007322.

*J.S.-V., C.E., and V.B. contributed equally to this study.

†I.S., E.S.J., and L.Q.-M. supervised the work equally.

The copy number and gene expression data reported in this article have been deposited in the Gene Expression Omnibus database (accession number GSE154834). Sequencing data have been deposited in the European Nucleotide Archive (accession number PRJEB42397). The corresponding author may be contacted for other forms of data sharing (e-mail: leticia.quintanilla-fend@med.uni-tuebingen.de).

The full-text version of this article contains a data supplement.

Introduction

Pediatric-type follicular lymphoma (PTFL) and pediatric nodal marginal zone lymphoma (PNMZL) are rare indolent B-cell lymphomas that occur predominantly in male subjects and frequently involve the head and neck region.[1,2] Unlike their adult counterparts, these lymphomas are characterized by localized disease and an excellent prognosis without systemic treatment.

The histopathologic distinction between these 2 entities is based on assessment of the nodal architecture and immunophenotype of the atypical cells. In PNMZL, the atypical cells are interfollicular and are negative for markers of follicle center derivation such as CD10 and BCL6.[1] In contrast, PTFL is characterized by expanded and serpiginous follicles, often with monomorphic centroblast-like cytology, with expression of CD10 and BCL6.[2] However, marginal zone differentiation has been reported in PTFL,[2-4] and we and others have noted cases that display intermediate features between both entities, making definitive categorization as PTFL or PNMZL on a morphologic basis challenging.

Studies of the genetic profile of nodal marginal zone lymphoma (NMZL) in adult patients have shown recurrent mutations in genes, including *KMT2D, TNFAIP3*, *NOTCH2*, *KLF2*, and *PTPRD*, in addition to frequent copy number (CN) alterations such as trisomies 3, 12, and 18.[5,6] The genetic landscape of PTFL is also well characterized as exhibiting very low genomic complexity,[7] frequent mutations in *MAP2K1*,[8,9] alterations targeting the *TNFRSF14* locus,[7,9,10] and *IRF8* p.K66R mutations.[8,11] In contrast, due to the low incidence of PNMZL, very few studies have been performed to analyze its genetic profile. In a previous study performed using fluorescence *in situ* hybridization (FISH), trisomy 18 and, occasionally, trisomy 3 were reported in PNMZL cases[12]; in a whole-exome sequencing (WES) analysis of 6 PNMZL cases, no recurrently mutated genes were identified.[11] We sought to characterize the genomic landscape of PNMZL to better understand the pathogenesis of this neoplasm and its relationship to PTFL and NMZL as seen in adults.

Materials and methods

Patients and samples

Forty-five cases with the diagnosis of PNMZL according to the World Health Organization lymphoma classification[13] were collected from the National Cancer Institute, National Institutes of Health (Bethesda, MD; 30 cases), University of Tübingen (Tübingen, Germany; 6 cases), Hospital Clínic of Barcelona (Barcelona, Spain; 3 cases), Universitätsklinikum Schleswig–Holstein (Kiel, Germany; 4 cases), and Samsung Medical Center (Seoul, South Korea; 2 cases). Cases were reviewed by 5 hematopathologists (C.E., S.P., E.C., L.Q.-M., and E.S.J.) blinded to the molecular results, and consensus diagnosis was achieved. Lymph node biopsy specimens were evaluated with hematoxylin and eosin. The immunohistochemical staining was performed as part of the diagnostic workup, including CD20, CD3, CD79a, CD10, BCL6, MUM1/IRF4, CD21/CD23, IgD, kappa, and lambda. Eleven cases (cases 34-44) were part of previously reported studies without mutational analysis.[1,12] Morphologically, all cases were estimated to have >30% tumor cells. For comparison, a previously published series of PTFL[7,8] were included for the methylation analysis and *IRF8* mutational status. In addition, 5 age-matched cases (patients aged 4-15 years) of reactive hyperplasia (RH), either atypical marginal zone hyperplasia (n = 4) or progressive transformation of germinal centers (n = 1), were included as controls (Table 1).

This study was approved by the institutional review boards of collaborating institutions and was conducted in accordance with the Declaration of Helsinki.

DNA extraction and clonality analysis

Genomic DNA was extracted from formalin-fixed paraffin embedded (FFPE) tissue sections with a Maxwell 16 FFPE Tissue LEV DNA Purification Kit or Maxwell RSC DNA FFPE Kit and the Maxwell 16 Instrument or the Maxwell RSC Instrument (Promega, Madison, WI) according to the manufacturer's protocol.

Polymerase chain reaction amplifications for detecting clonal IGH and/or IGK chain gene rearrangements were performed according to the BIOMED-2 protocol (supplemental methods).[7,14]

Copy number analysis

Forty-six DNA samples (from 42 tumors and 4 control specimens) were hybridized on OncoScan and 3 samples (2 cases and 1 RH) on CytoScan arrays (Thermo Fisher Scientific, Waltham, MA) following standard protocols. Gains, losses, and copy number–neutral loss of heterozygosity (CNN-LOH) regions were evaluated and visually inspected by using Nexus BioDiscovery version 9.0 software (BioDiscovery, Hawthorne, CA) aligning to human reference genome GRCh37/hg19.

WES analysis

WES analysis was performed on four PNMZL samples with high-quality DNA available (supplemental Figure 1), including 3 unpaired FFPE samples and 1 frozen tissue sample with a paired normal peripheral blood sample. For the frozen tissue and peripheral blood samples, libraries were created by using the SureSelect Human All Exon V5 50-Mb target enrichment kit (Agilent Technologies, Santa Clara, CA)[15] and were sequenced on a HiSeq 2000 instrument (Illumina, San Diego, CA). For the FFPE samples, libraries were generated by using the Agilent SureSelect V6 exome target enrichment kit and were sequenced on a HiSeq 4000 Illumina instrument (Illumina). The variant filtering pipeline is detailed in the supplemental Methods.

Targeted next-generation sequencing analysis

Targeted next-generation sequencing (NGS) analysis was performed on the Ion Torrent PGM and Ion GeneStudio S5 Prime (Thermo Fisher Scientific) system. NGS libraries were amplified by using two or three primer pools of four Ion AmpliSeq Custom Panels covering 27 genes that have been shown to be mutated in follicular lymphoma, PTFL (NGS1, NGS2, and NGS3 panels) (supplemental Tables 1-3),[8,16-18] and adult NMZL (NGS4 panel) (supplemental Table 4).[5,6] The custom panels were designed by using the Ion AmpliSeq Designer from Thermo Fisher Scientific (NGS1 panel version 3.0, NGS2 panel version 3.4, NGS3 panel version 7.49, and NGS4 panel version 5.6.2) to interrogate all exons of 19 genes (*EP300*, *FOXO1*, *GNA13*, *HIST1H1B*, *HIST1H1C*, *HIST1H1D*, *HIST1H1E*, *IRF8*, *KMT2D*, *MEF2B*, *TNFRSF14*, *TNFAIP3*, *STAT6*, *SOCS1*, *KLF2*, *NOTCH3*, *PTPRD*, *TET2*, and *TBL1XR1*) and selected regions of 8 genes (*CREBBP*, *EZH2*, *XPO1*, *NOTCH1*, *NOTCH2*, *MYD88*, *MAP2K1,* and *BRAF*)

Table 1. Clinical, morphologic, and IG clonality features of 45 cases with the diagnosis of PNMZL

Case no.	Age, y	Sex	Lymph node biopsy site	Original diagnosis	Overlapping features	IG gene rearrangement studies
1	16	M	Preauricular	PNMZL	Yes	Monoclonal
2	20	M	Parotid	PNMZL	Yes	Monoclonal
3	18	M	Cervical	PNMZL	No	Monoclonal
4	12	M	Submandibular	PNMZL	Yes	Monoclonal
5	20	F	Occiput	PNMZL	Yes	Monoclonal
6	15	M	Posterior cervical	PNMZL	Yes	Monoclonal
8	14	F	Cervical	PNMZL	No	Monoclonal
9	23	M	Submental	PNMZL	Yes	Monoclonal
10	18	M	Inguinal	Overlapping features of PNMZL and PTFL	Yes	Monoclonal
11	12	M	Right inguinal	Overlapping features of PNMZL and PTFL	Yes	Monoclonal
12	15	M	Scalp	Overlapping features of PNMZL and PTFL	Yes	Monoclonal
13	23	M	Cervical	Overlapping features of PNMZL and PTFL	Yes	Monoclonal
14	20	F	Inguinal	Overlapping features of PNMZL and PTFL	Yes	Monoclonal
15	20	M	Submental	PNMZL	No	Monoclonal
17	20	M	Parotid	PNMZL	No	Monoclonal
19	9	M	Parotid	Overlapping features of PNMZL and PTFL	Yes	Monoclonal
21	9	M	Cervical	PNMZL	No	Monoclonal
23	16	M	Right cervical	Overlapping features of PNMZL and PTFL	Yes	Monoclonal
25	5	M	Cervical	PNMZL	No	Monoclonal
27	6	M	Cervical	PNMZL	Yes	Monoclonal
28	5	M	Left inguinal	PNMZL	Yes	Monoclonal
29	8	M	Submandibular	PNMZL	No	Monoclonal
31	16	M	Parotid	Overlapping features of PNMZL and PTFL	Yes	Monoclonal
34	18	M	Left cervical	PNMZL	Yes	Monoclonal
35	6	M	Axilla	PNMZL	Yes	Monoclonal
36	22	M	Cervical	PNMZL	No	Monoclonal
37	16	M	Right inguinal	PNMZL	No	Monoclonal
38	17	M	Submental	PNMZL	Yes	Monoclonal
39	22	M	Submental/cervical	PNMZL	Yes	Monoclonal
40	16	M	Cervical	PNMZL	Yes	Monoclonal
41	14	M	Left cervical	PNMZL	Yes	Monoclonal*
42	6	M	Right cervical	PNMZL	Yes	Monoclonal
43	23	M	Supraclavicular	PNMZL	Yes	Monoclonal
44	15	M	Right inguinal	PNMZL	Yes	Monoclonal
45	13	M	Right cervical	PNMZL	No	Monoclonal
46	19	M	Cervical	PNMZL	Yes	Monoclonal
47	17	M	Left cervical	PNMZL	No	Monoclonal
48	11	M	Right postauricular	PNMZL	No	Monoclonal
49	11	M	Inguinal	Overlapping features of PNMZL and PTFL	Yes	Monoclonal
50	28	M	Cervical	Overlapping features of PNMZL and PTFL	Yes	Monoclonal
51	15	F	Cervical	Overlapping features of PNMZL and PTFL	Yes	Monoclonal
52	16	M	Cervical	Overlapping features of PNMZL and PTFL	Yes	Insufficient DNA quality
54	15	M	Cervical	Overlapping features of PNMZL and PTFL	Yes	Monoclonal
55	30	M	Inguinal	PNMZL	No	Monoclonal
58	14	F	Right cervical	PNMZL	No	Monoclonal

IG, immunoglobulin; M, male; F, female; LN, lymph node; NA, not applicable.
*An IGK clone was detected and confirmed by using NGS-based analysis (data not shown).

Table 1. (continued)

Case no.	Age, y	Sex	Lymph node biopsy site	Original diagnosis	Overlapping features	IG gene rearrangement studies
Control 1	15	M	Cervical	Atypical marginal zone hyperplasia	NA	Polyclonal
Control 2	13	M	Cervical	Atypical marginal zone hyperplasia	NA	Polyclonal
Control 3	18	M	Cervical	Atypical marginal zone hyperplasia	NA	Polyclonal
Control 5	7	F	Cervical	Progressive transformation of germinal centers	NA	Polyclonal
Control 6	4	F	Cervical	Atypical marginal zone hyperplasia	NA	Polyclonal

IG, immunoglobulin; M, male; F, female; LN, lymph node; NA, not applicable.
*An IGK clone was detected and confirmed by using NGS-based analysis (data not shown).

(supplemental Tables 1-4). For comparison, 37 PTFLs were analyzed for *IRF8* using the NGS3 panel. A description of library preparation, sequencing, and raw data analyses is presented in the supplemental Methods.

Targeted resequencing and Sanger sequencing

For validation of the NGS results, selected variants with low allelic frequencies (<15%) were re-analyzed as single amplicons using a targeted resequencing approach or using another NGS panel on the Ion Torrent PGM or Ion GeneStudio S5 Prime system. A description of primer design is presented in the supplemental Methods and supplemental Table 5.

DNA methylation analyses

DNA methylation analyses were performed on a total of 22 PNMZL cases and 26 previously published PTFL cases[7] using the Infinium MethylationEPIC BeadChip (Illumina) according to the manufacturer's instructions. Bisulfite conversion of genomic DNA was

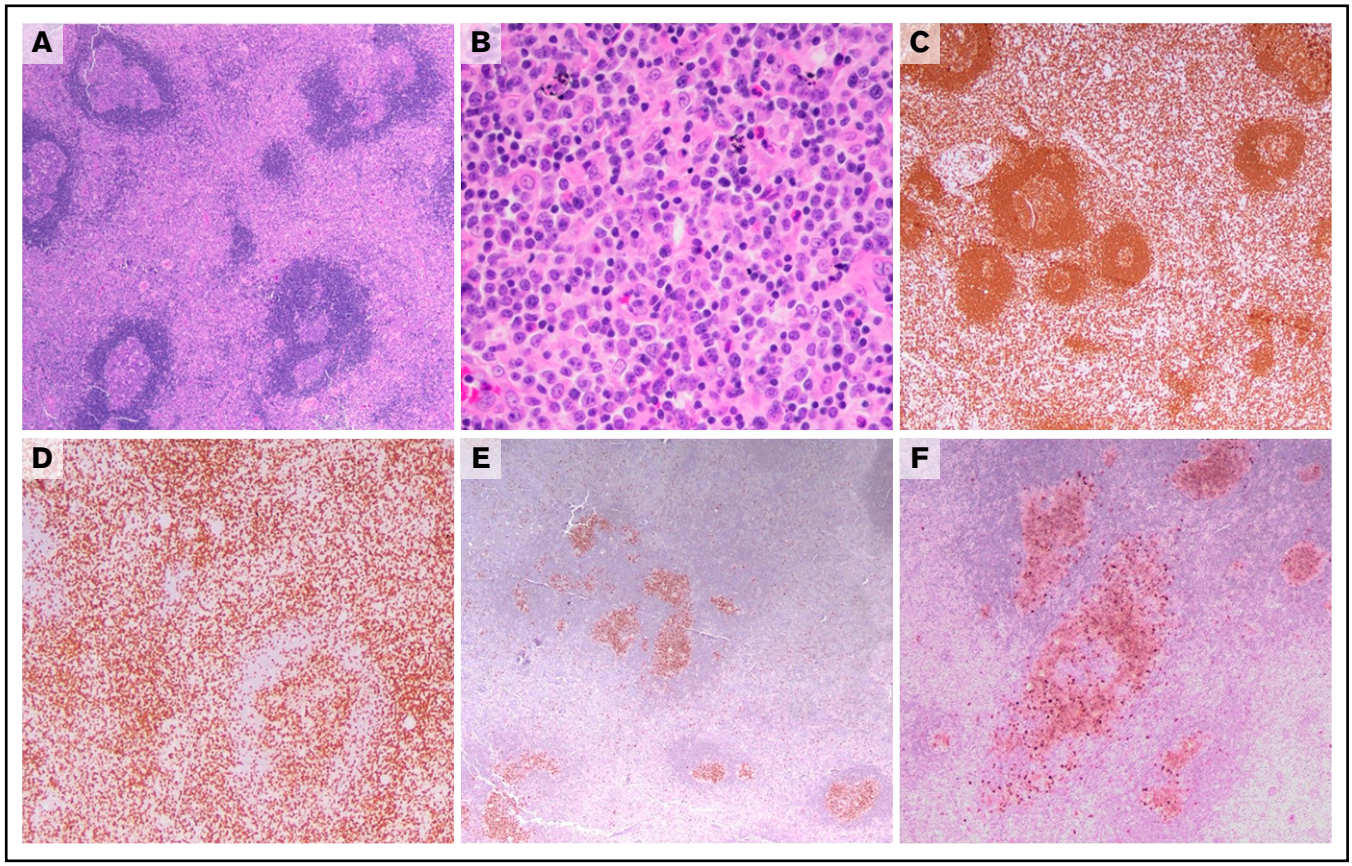

Figure 1. PNMZL with features reminiscent of PTFL. (A) The lymph node shows scattered large follicles with intact mantle cuffs. The germinal centers are irregular and fragmented, resembling progressive transformation of germinal centers. However, the interfollicular region is markedly expanded. (B) The atypical interfollicular infiltrate is polymorphous and is composed of small- to medium-sized lymphoid cells, some displaying plasmacytoid features. Occasional eosinophils and histiocytes are present. (C) The CD20 stain highlights increased interfollicular B cells. (D) CD3 shows admixed T cells, some of which localize to the follicle centers. BCL6 highlights the germinal centers (E), some of which show an irregular serpiginous configuration also seen with the stain for CD10 (F).

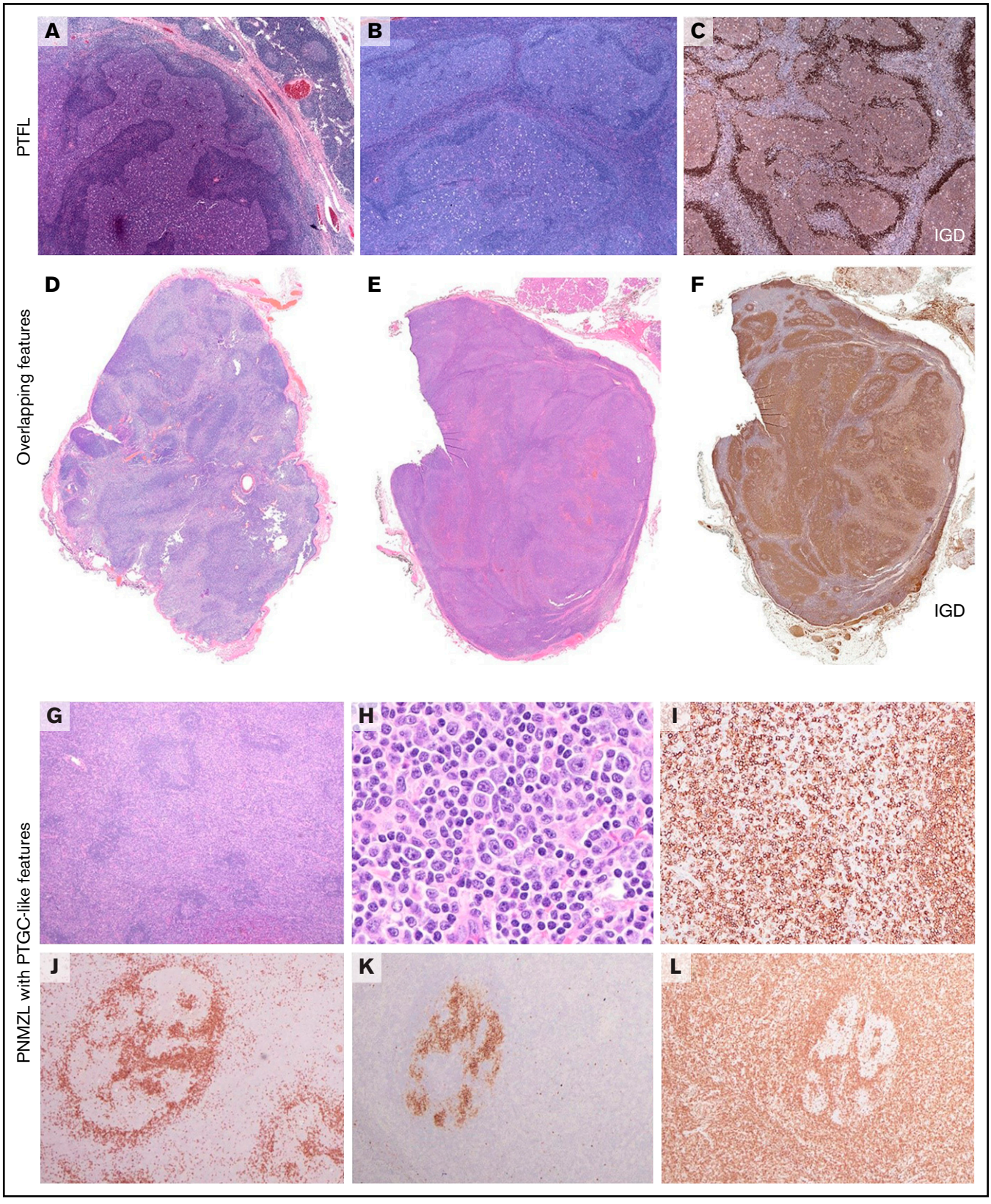

Figure 2. Morphological characteristics of PTFL, PNMZL and cases with overlapping features. (A-B) Two examples of typical PTFL with expanded, serpiginous germinal centers with a starry-sky pattern and attenuated mantle zones. Note in panel A, a rim of normal lymph node at the upper edge of the biopsy specimen. (C) IgD stain highlights the attenuated mantle zone. (D) PNMZL with overlapping features with PTFL, Case 28. The lymph node shows large, irregular germinal centers with attenuated

performed applying the EZ DNA Methylation kit (Zymo Research, Irvine, CA) according to the protocol supplied by the manufacturer. DNA methylation data were processed by using GenomeStudio software (version 2011.1; methylation module 1.9.0; Illumina) and Qlucore Omics Explorer version 3.6 (Qlucore, Lund, Sweden), applying the default settings as previously described.[19] The intrinsic controls present on the array were used for data normalization. Single nucleotide polymorphism loci, loci on gonosomes, and loci with a detection P value $>.01$ were excluded from further analysis.

Statistical analyses

R software version 3.6.2 (R Foundation for Statistical Computing, Vienna, Austria) was used for statistical analysis. Differences in the distribution of individual parameters among patient subsets were analyzed by using Fisher's exact test for categorical variables and a t-test for continuous variables. The nonparametric Wilcoxon test was applied when necessary. P values for multiple comparisons were adjusted by using the Benjamini-Hochberg correction (false discovery rate). A cutoff of $P = .05$ was considered significant unless otherwise indicated.

Results

Clinical characteristics and morphologic findings

The clinical characteristics of the cases are summarized in Table 1. There were 45 cases in total from a cohort of 40 males and 5 females with a median age of 16 years (range, 5-30 years). The most common anatomic sites of presentation were in cervical lymph nodes (n = 22 [49%]), with other sites of involvement including inguinal (n = 8 [18%]), submental (n = 5 [11%]), intraparotideal (n = 4 [9%]), periauricular, occipital (n = 2 each [4%]), and supraclavicular and axillary (n = 1 each [2%]) regions. All patients presented with a single anatomic site of disease (stage I).

Most of the cases were originally diagnosed as PNMZL (n = 32), with a smaller number initially appreciated to show some overlapping features between PNMZL and PTFL (n = 13). Characteristic features of PNMZL included interfollicular expansion by a polymorphous lymphoid infiltrate composed of small- to medium-sized lymphoid cells with pale cytoplasm and focal plasmacytoid differentiation. Dutcher bodies were absent. Follicular structures were always present but to a varying degree and extent, with the interfollicular component occupying most of the lymph node surface area. However, in most cases, the interfollicular component encroached upon the follicles, with frequent disruption of the mantle cuffs and fragmentation of the follicle centers, producing a histologic picture resembling progressive transformation of germinal centers that has been defined as a feature of PNMZL (Figure 1).[1,13]

According to immunohistochemistry, the follicle centers were strongly positive for BCL6 and CD10, and negative for BCL2. The interfollicular component was consistently negative for these germinal center markers. The mantle cuffs were highlighted by IgD and were generally broad, to a greater extent than typically observed in PTFL. However, in many cases, the follicular component was present in much of the node, with the polymorphous and monocytoid cells forming broad coronas around the follicles. Based on the extent of the follicular component, a total of 31 cases (69%) were considered to have overlapping features between PNMZL and PTFL after central consensus review. However, cases classified as PNMZL always had a dominant interfollicular and polymorphous B-cell expansion, with only a minor follicular component. A comparison of the histologic features between PTFL and PNMZL with "overlap" is presented in Figure 2.

IG clonality and CN and CNN-LOH alterations in PNMZL and RH

Immunglobulin (IG) gene rearrangement was monoclonal in all 44 cases analyzed. The 5 cases of RH used as controls rendered polyclonal results with all IG primer sets used (Table 1).

The CN profile of 44 PNMZL and five RH cases was investigated. Tumor samples showed a total of 53 copy number alterations (CNA) in 20 of 44 cases (mean, 1.2 alterations per case; range, 0-18 alterations) (Figure 3A; supplemental Table 6), and 8 of 24 cases with no CNA displayed CNN-LOH as the sole abnormality. Thirty-six regions of CNN-LOH were detected in 15 of 44 cases (Figure 3B). The most recurrently altered locus was 1p36, including *TNFRSF14*, with 4 cases showing CNN-LOH and one additional case harboring a deletion of 1p36. In addition, CN gains of 3q26.32-q29, 11p15.5-q22.1, and 12p arm were found in 3 cases. Previously reported trisomies of chromosomes 3 and 18 were only detected in one case each, indicating that these alterations are rare in PNMZL.[12]

All RH control samples analyzed displayed no alterations except for one carrying a CN gain (3q13.31-q13.32) of uncertain significance (supplemental Table 6).

PNMZL WES analysis

Four selected cases (one with frozen tissue and paired normal DNA and three FFPE samples with DNA quality above 400 bp) were analyzed by using WES. This procedure yielded a mean coverage of 133.9× (range, 118.2-155.7). After filtering, a total of 32 variants were detected in the 4 analyzed cases (mean, 8 alterations per case; range, 1-11 alterations) (supplemental Tables 7 and 8), with 15 predicted to be potentially driver alterations according to previously published criteria.[20] Only the *MAP2K1* gene was found to be mutated in 2 cases.

Identification of recurrent mutations by targeted NGS

All 45 cases were analyzed by using targeted NGS (Figures 4-5). Twenty-five cases were informative with all 4 gene panels, and 6 cases were informative with 3 panels. Fourteen cases with low

Figure 2 (continued) marginal zones together with expanded interfollicular areas. (E) Case 19. The lymph node reveals an infiltrate with nodular pattern with recognizable hyperplastic germinal centers and expanded mantle zones with marginal differentiation. (F) IgD stain shows the extension of the mantle zone B cells into the germinal centers, which display fragmentation, resembling progressively transformed germinal centers (PTGC). (G-L) PNMZL with PTGC-like features.Case 40. (G) Lymph node with residual reactive follicles but the interfollicular region is markedly expanded. (H) The cellular infiltrate is polymorphous with occasional plasma cells and immunoblasts. (I) A stain for CD20 shows a predominance of B cells surrounding a residual follicle. (J) IgD stain shows the intact mantle cuff. The germinal center exhibits some fragmentation reminiscent of PTGC. (K) The residual germinal centers are positive for CD10 and negative in the atypical cells. (L) BCL2 is negative in germinal centers but positive in interfollicular cells.

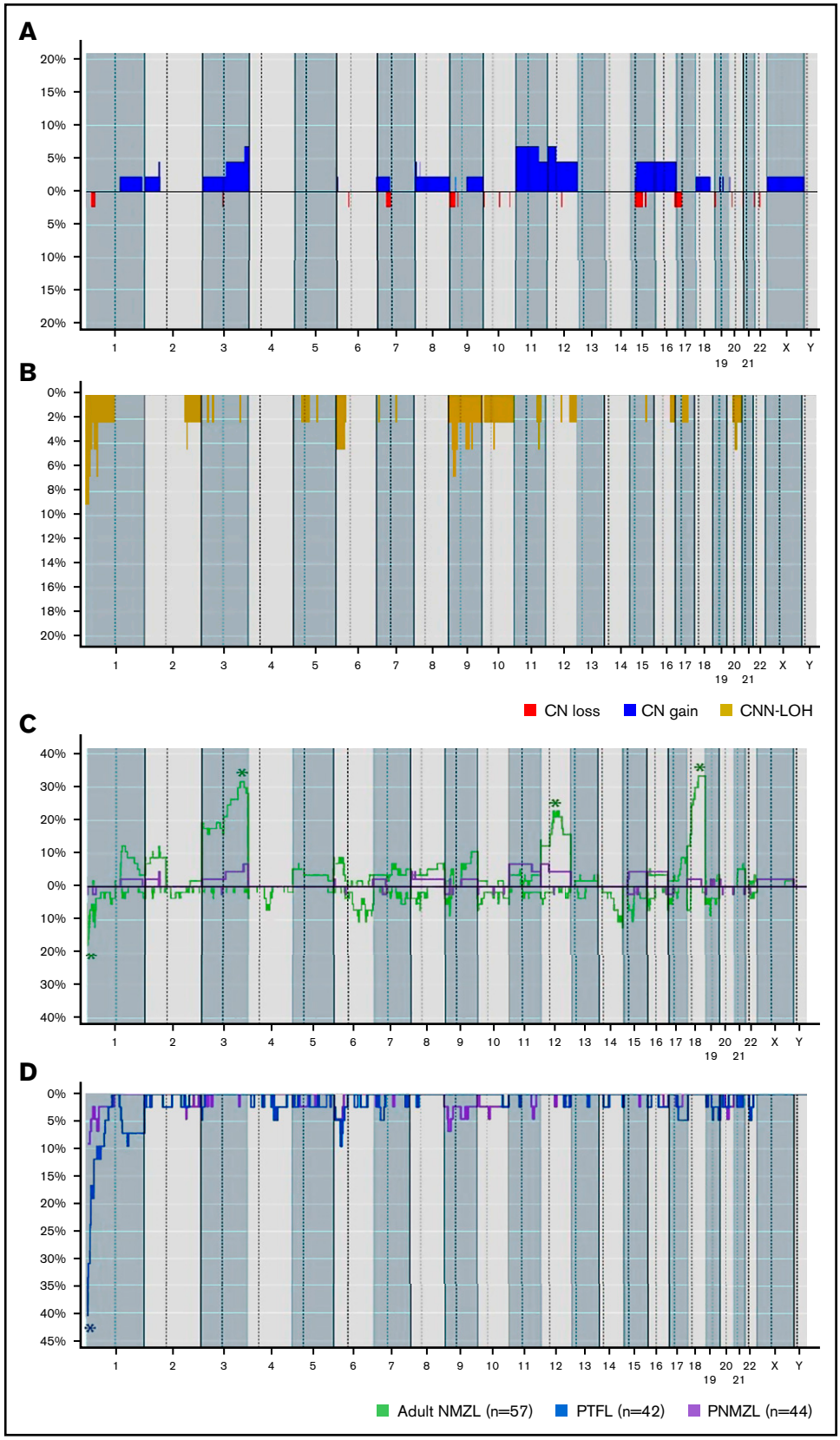

Figure 3. Global CN and CNN-LOH profiles of 44 PNMZL cases and comparison plots with CN data from adult NMZL and CNN-LOH data from PTFL. (A-B) Global CN alterations and CNN-LOH profiles in 44 PNMZL cases. (C) Comparison of CN alterations between adult NMZL (57 cases) and PNMZL (44 cases). (D) Comparison of CNN-LOH regions between PNMZL (44 cases) and PTFL (42 cases). The horizontal axis indicates chromosomes from 1 to Y and from arm p to q. The vertical axis represents the frequency of the genomic event among the analyzed cases. CN gains are depicted in blue, CN losses in red, and CNN-LOH in yellow

DNA quality (≤200 bp) were informative at least for 2 panels. The mean read depth of the NGS sequence analysis was 8763 for mutations (range, 576-59 079). In the 45 cases, 60 mutations were identified (supplemental Table 9) with a mean of 1.3 mutations per case. Fifty-seven (95%) of 60 mutations were validated with targeted single amplicons (35 mutations) or with a different NGS panel (20 mutations) with a verification rate of 100%. The most frequently mutated gene was *MAP2K1* with 22 mutations in 19 cases (2 mutations in cases 12, 19, and 25; 19 of 45 [42%]) and a median variant allele frequency of 9% (range, 3%-27%), followed by *TNFRSF14* with 16 mutations in 13 patients (2 mutations in cases 2, 9, and 12; 13 of 36 [36%]) and a median variant allele frequency of 18% (range, 4%-50%), and *IRF8* with 16 mutations in 12 cases (2 mutations in cases 2, 31, 34, and 45; 12 of 35 [34%]) and a median variant allele frequency of 5% (range, 1%-13%). Additional mutated genes were *EZH2* (2 of 31 [6%]), *FOXO1* (1 of 31 [3%]), *GNA13* (1 of 31 [3%]), *HIST1H1C* (1 of 31 [3%]), and *HIST1H1D* (1 of 31 [3%]). No mutations were identified in *CREBBP, EP300, HIST1H1B, HIST1H1E, KMT2D, MEF2B, STAT6, XPO1, MYD88*, *SOCS1, TNFAIP3, NOTCH1, NOTCH2, NOTCH3, KLF2, PTPRD, BRAF, TET2*, and *TBL1XR1* genes.

MAP2K1 gene mutations were nonsynonymous and targeted mainly the negative regulatory region domain of MEK1 protein. The most common recurrent mutations clustered in exon 2, hot spot codon 53 found in 12 cases (12 of 19 [63%]), and codon 57 found in 3 cases (3 of 19 [16%]) (Figure 4A). *TNFRSF14* gene mutations included 11 missense mutations, 2 stop variants, 1 frameshift mutation, and 2 intronic variants. These mutations were found in the first 4 exons coding for the signal peptide and part of the extracellular domain containing the tumor necrosis factor (TNF) receptor (TNFR) cysteine repeats 1 and 2 (Figure 4B). *IRF8* mutations were not restricted to the hot spot K66 (7 of 16 [44%]), with recurrent mutations targeting codon 23 (p.Y23H) also identified (5 of 16 [31%]) (Figure 4C). In total, *MAP2K1, TNFRSF14*, and/or *IRF8* mutations were observed in 30 (73%) of 41 cases, and 11 cases showed concomitant mutations of these genes. Cases with overlapping morphology more often carried mutations of these 3 genes (22 of 28 [78.5%]) compared with those cases with PNMZL morphology (8 of 13 [61.5%]); however, the difference was not statistically significant ($P = .2802$). In contrast, no mutations were identified in the 5 lymph nodes with RH used as controls.

All except for 1 case were investigated by using both CN and mutational analysis. The integrated CN and mutational information (Figure 5) revealed that the most recurrently mutated gene was *MAP2K1* (42% [19 of 45 cases]), followed by *IRF8* (34% [12 of 35 cases]) and frequent alterations in 1p36/*TNFRSF14* locus (33% [15 of 45 cases]). *TNFRSF14* mutations occurred concomitantly with 1p36 CNN-LOH in 2 cases and with 1p36 CN loss in 1 case. Twelve (27%) of 45 cases lacked CNA and gene mutations.

Genetic comparison of PNMZL with NMZL and PTFL

To compare PNMZL with NMZL in the adult population, previously published CN raw data were reanalyzed following the same criteria used for PNZML data analysis.[5,6] PNMZL exhibits a lower genetic complexity than adult NMZL (mean, 1.2 CNA per case vs 6.1 CNA per case; $P < .001$) and lacks the CNA typically found in adult NMZL such as trisomies 3, 12, and 18, and CN loss of 1p36 locus ($P < .05$) (Figure 3C). Comparison of the mutational profile of PNMZL with previously published mutational information from adult NMZL[5,6] showed that *MAP2K1* and *IRF8* mutations are exclusively found in the pediatric group (adjusted $P < .05$). Furthermore, mutations frequently found in adult NMZL affecting genes, including *KMT2D*, *KLF2, TBL1XR1, NOTCH2*, and *TNFAIP3*, were absent in PNMZL (adjusted $P < 0.05$) (Figure 6A).

Comparison of PNMZL with PTFL was performed by using previously published CN data on PTFL.[7] Statistical analyses showed that both entities have a similar level of genetic complexity (mean, 1.2 CNA per case in PNMZL vs 0.7 CNA per case in PTFL). In general, PTFL cases showed more CNN-LOH alterations than PNMZL cases (mean, 0.8 CNN-LOH alterations per case in PNMZL vs 1.8 CNN-LOH alterations per case in PTFL; $P < .01$). Moreover, both groups showed 1p36 CNN-LOH, but this alteration was more frequently observed in PTFL (9% of cases in PNMZL vs 40% of cases in PTFL; $P < .05$) (Figure 3D). No differences were observed between PNMZL and cases with overlapping features (supplemental Figure 2). Comparative analyses of the mutational landscape of PTFL with PNMZL and overlapping cases were also performed by using published data on PTFL.[7] In addition, to compare the *IRF8* mutational status among the 3 groups, 37 PTFL cases were analyzed by using the same NGS approach. The analysis showed that the 3 groups have a similar mutational landscape but with different frequencies (Figure 6B; Table 2). *EZH2* mutations were only observed in PNMZL ($P < .05$).

Methylation profile of PNMZL

Unsupervised hierarchical cluster analysis of all investigated samples did not clearly differentiate PNMZL and PTFL into unique clusters but resulted in considerable overlap of the 2 groups (supplemental Figure 3). Supervised hierarchical cluster analysis, according to the original diagnosis and the diagnosis after review, also showed no clear separation of each entity. Therefore, 2-group comparison (*t*-test, $\sigma/\sigma max \geq 0.4$; $q \leq 0.01$) as well as multiple-group comparison (analysis of variance, $\sigma/\sigma max \geq 0.4$; $q \leq 0.01$), including the samples with overlapping features of both entities, were performed (supplemental Figure 4). Supervised analysis of both multiple-group comparisons (original diagnosis and after review) revealed 28 and 29 CpGs, respectively, to be differently methylated, affecting 19 genes (supplemental Figures 4 and 5). Gene ontology analysis of these differentially methylated CpGs suggested an unspecific cancer effect rather than a specific role in B-cell lymphomagenesis (supplemental Table 10).

Figure 3 (continued) (in panel C, upward representing CN gains and downward representing CN losses). CN and CNN-LOH data from PNMZL are depicted in purple, CN data from adult NMZL are depicted in green, and CNN-LOH data from PTFL are depicted in blue. Asterisks mark regions with statistically significant differences among groups after applying Fisher's exact test adjusted; *P* value < .05, and considering, minimum, 5 altered cases.

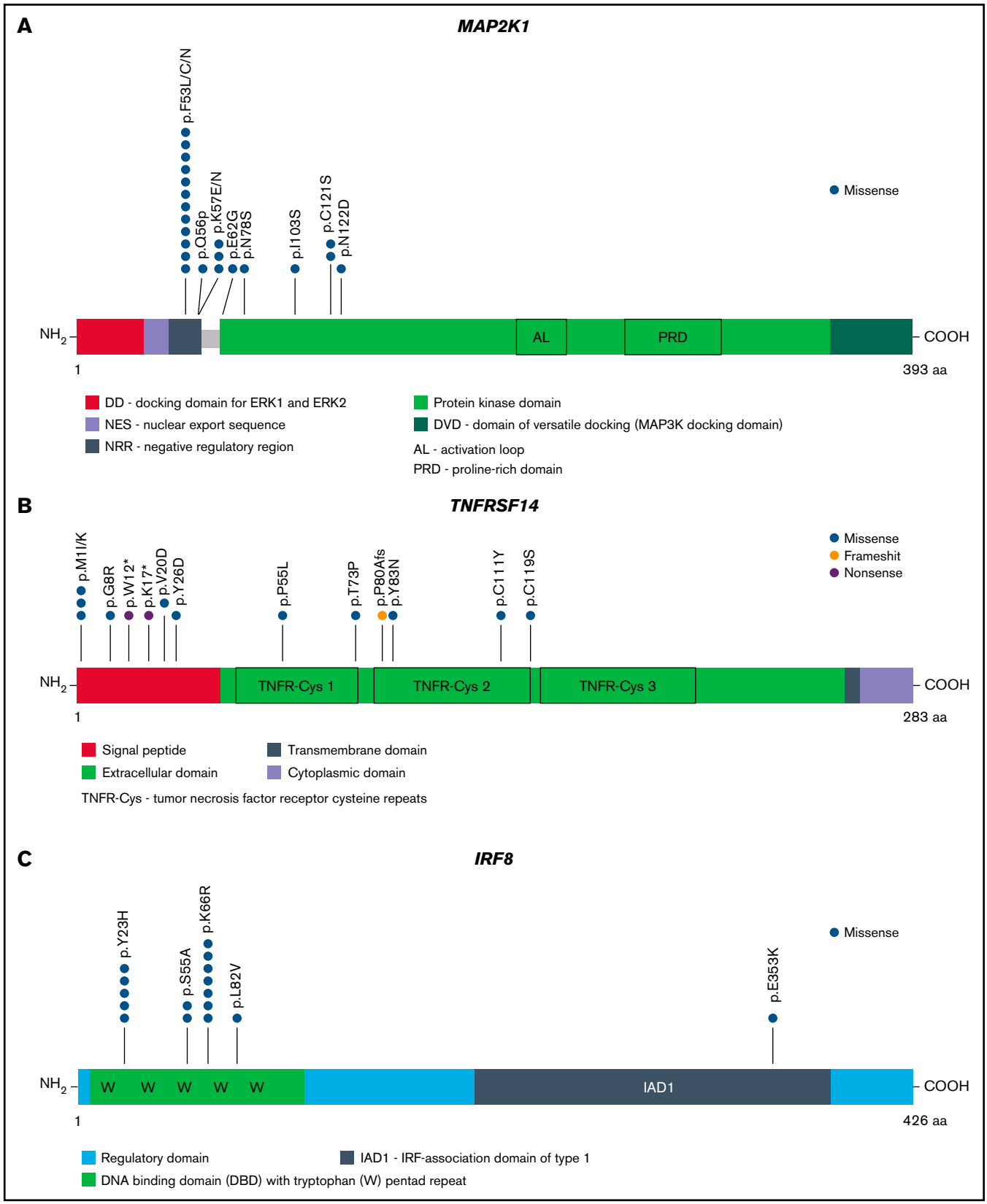

Figure 4. Frequent mutations in PNMZL and mutational comparison between adult NMZL and PNMZL. (A) Distribution of *MAP2K1* mutations at protein level. The main protein domains are represented by larger colored boxes. (B) Distribution of *TNFRSF14* mutations at protein level. Intron variants are not shown. (C) Distribution of *IRF8* mutations at protein level. Domains of the protein are represented according to the UniProt database (www.uniprot.org).

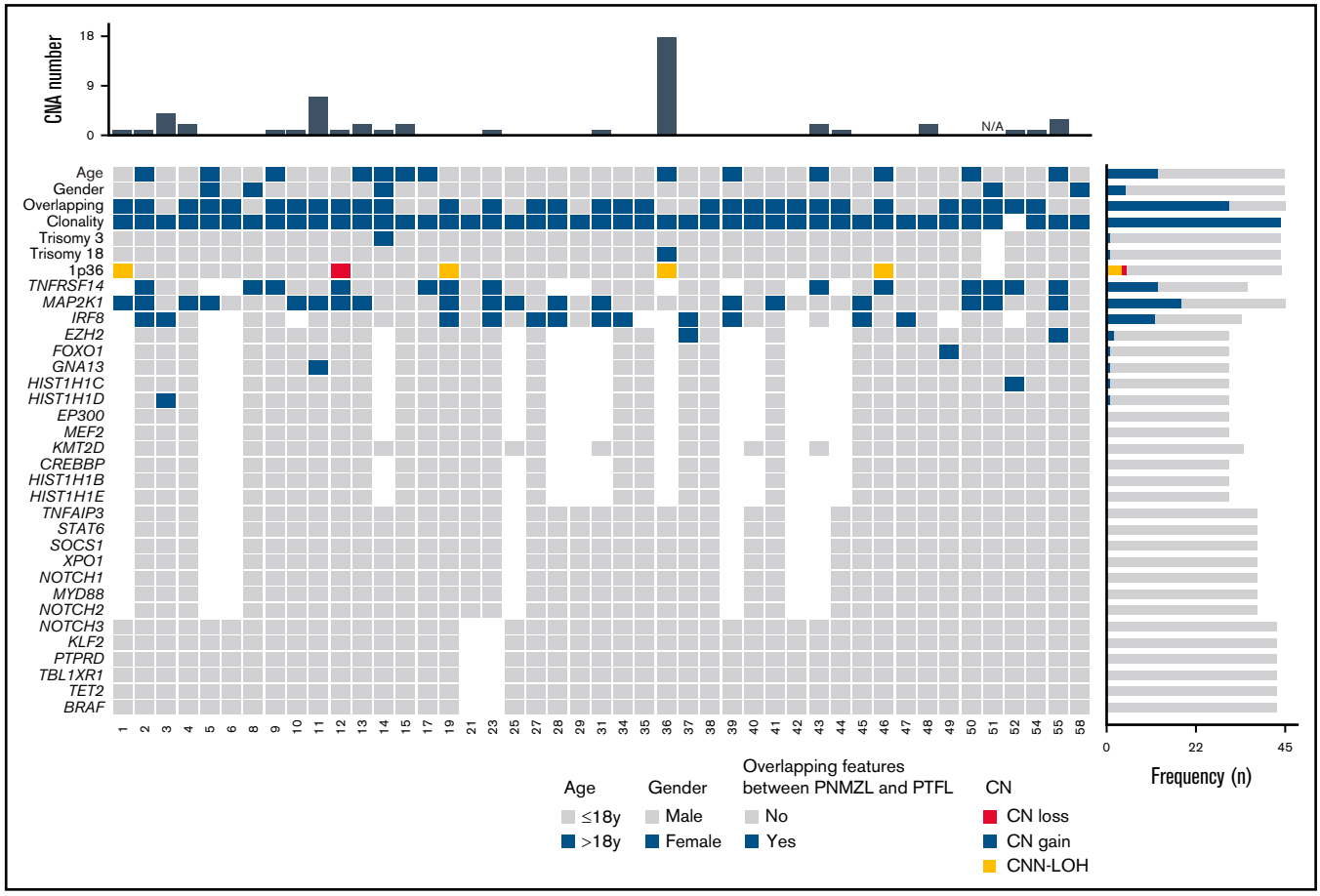

Figure 5. Overview of the CN and mutational profile of 45 PNMZL analyzed. Each column of the heatmap represents a case, and each row represents an analyzed variable. The right histogram represents the frequency of the variable in question. For CN, blue indicates CN gain, red indicates CN loss, and green indicates CNN-LOH. For clonality, blue represents monoclonal cases. Absent blocks indicate information not available.

Discussion

PNMZL is a mature B-cell lymphoma seen mainly in children and young adults, which commonly occurs with localized disease in the head and neck region of adolescent boys. It has long been recognized that PNMZL displays similarities with PTFL in terms of epidemiology, clinical presentation, and pathologic features[21,22]; however, recurrent abnormalities in PNMZL have not been described, in contrast to the well-characterized mutational landscape of PTFL. To the best of our knowledge, this study is the first to perform molecular analysis on a large series of PNMZL using an integrated approach, including targeted NGS, CN, and methylation arrays. We now show that in addition to clinical and morphologic overlap, PNMZL exhibits similarities to PTFL on a molecular level but is distinct from adult-type NMZL.

To identify novel mutated genes specific to PNMZL, WES was performed on 4 cases. This analysis identified only recurrent *MAP2K1* mutations in 2 cases. Because WES analysis did not provide new possible candidate genes besides *MAP2K1*, targeted NGS panels were additionally designed to interrogate genes that have been previously described as mutated in adult-type NMZL,[5] conventional follicular lymphoma,[16-18] and PTFL.[8] Interestingly, this analysis showed that the mutational profile of PNMZL cases was similar to that of PTFL, identifying *MAP2K1* (19 of 45 [42%]), *TNFRSF14* (13 of 36 [36%]), and *IRF8* (12 of 35 [34%]) as the most frequently mutated genes. The functional impact of *MAP2K1* mutations has been previously investigated by immunohistochemistry with the presence of phosphorylated extracellular signal-regulated kinase confirming the expected activation of the extracellular signal-regulated kinase pathway.[8] *TNFRSF14* mutations, as reported in PTFL,[7] involve the binding sites of *TNFRFS14* to ligands, including members of the TNF superfamily (LTα and LIGHT) and the Ig superfamily members BTLA and CD160, which function as checkpoint regulators, suggesting that these mutations may affect ligand-binding activity.[23] The other important similarity was the presence of *IRF8* mutations, which are reportedly specific for PTFL in 15% to 50% of cases.[8,11] Interestingly, in addition to the hot spot K66 position (p.K66R; 7 of 16 [44%]), we now detected a second hot spot on codon 23 (p.Y23H; 5 of 16 [31%]), also targeting the DNA-binding domain. *TNFRSF14* and *IRF8* mutations co-occurred in 10% of the cases in both PNMZL and PTFL, suggesting possible cooperation between these 2 genes.[7] Indeed, both genes are involved in the regulation of immune system development and function and regulate germinal center B-cell activation.[24,25] Although the mutational profiles of PNMZL and PTFL are very similar, there was an important difference. *TNFRSF14* mutations were also frequently observed in PNMZL (36% vs 54%); however, in contrast to PTFL, *TNFRSF14* mutations were associated with 1p36 CNN-LOH or deletion in only

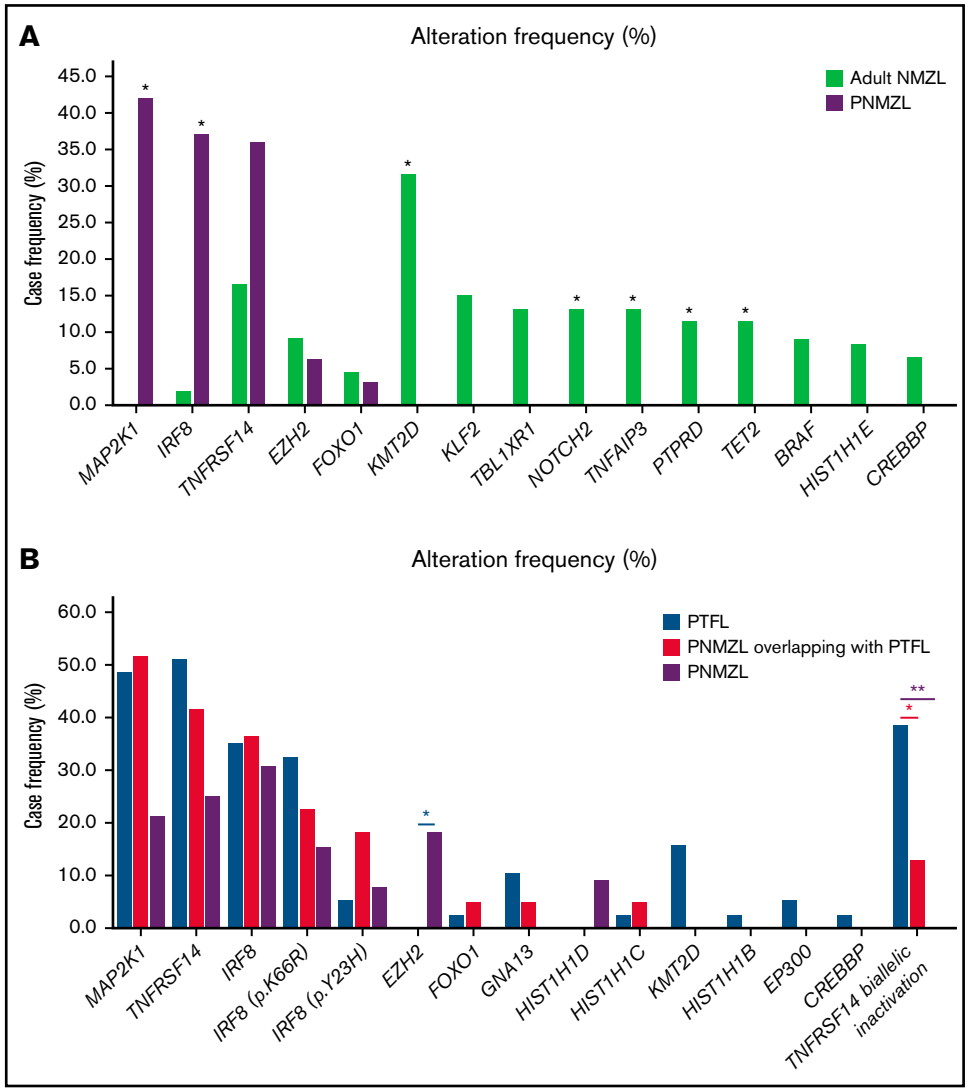

Figure 6. Comparison of alteration frequencies of PNMZL versus adult NMZL and PTFL. (A) Comparison of mutation frequency of genes recurrently mutated in PNMZL and in adult NMZL.[5,6] For statistical comparison, only frequently mutated genes (>5%) and regions analyzed in both groups were considered; that is, all coding sequence of *TNFRSF14*, *KMT2D*, *TBL1XR1*, *TNFAIP3*, and *HIST1H1E* and mutation hot spots of *MAP2K1*, *EZH2*, *FOXO1*, *TET2*, *BRAF*, *KLF2*, *NOTCH2*, *PTPRD*, and *CREBBP*. Genes are represented along the horizontal axis, and the mutation frequency is represented on the vertical axis. Adult NMZL is depicted in green, and PNMZL is depicted in purple. Asterisks mark statistically significant differences in the incidence of mutation (Fisher's exact test, *adjusted $P < .05$). (B) Comparison of alteration frequency of genes recurrently mutated in PNMZL, cases with overlapping features and PTFL.[8] Genes are represented along the horizontal axis, and the alteration frequency is represented on the vertical axis. PNMZL is depicted in purple, cases with overlapping features are represented in gray, and PTFL is depicted in blue. Asterisks mark statistically significant differences in the incidence of alteration, with colors indicating the group in which the frequency is significantly different (Fisher's exact test, *$P < .05$, **$P < .01$).

3 cases (9% vs 38%; adjusted $P < .05$).[8] A relatively recent study has shown that loss of *TNFRSF14* leads to activation of B-cell receptor–related proliferation signals that drive the development of germinal center lymphomas, and that disruption of *TNFRSF14* in lymphoma cells also induces tumor-supportive changes in the microenvironment, including increased recruitment of T-follicular helper cells and stromal activation.[24] The more frequent allelic dominance of mutated *TNFRSF14* might play a role in the prominence of neoplastic germinal centers observed in PTFL, as opposed to PNMZL.

The molecular analysis revealed that PNMZL has a similarly low level of genetic complexity as PTFL. Therefore, methylation profiling was performed as an additional analysis to investigate possible differences between PNMZL and PTFL. On a global scale, the DNA methylation profile did not explicitly differentiate each lymphoma subtype.

In contrast, our results clearly show that adult-type NMZL and PNMZL are genetically 2 different diseases. PNMZL exhibits a lower genetic complexity and lacks chromosomal alterations typically found in adult-type NMZL such as trisomies 3, 12, and 18. Notably, in a previous study based on the FISH technique, it was reported that PNMZL carried recurrent trisomy 18 (4 of 23 [17%]). In the current study, we did not corroborate this finding and identified only one trisomy 18 (1 of 44 [2%]). An explanation for this discrepancy

Table 2. Mutational profile of PNMZL and PNMZL with overlapping PTFL features, compared with previously reported mutations in PTFL

Gene	Alteration frequency in PTFL (cases)	Alteration frequency in PNMZL overlapping PTFL (cases)	*P*	Adjusted *P*	Alteration frequency in PNMZL (cases)	*P*	Adjusted *P*
MAP2K1	20/41 (48.8%)	16/31 (51.6%)	1.00	1.00	3/14 (21.4%)	.12	.58
TNFRSF14	21/41 (51.2%)	10/24 (41.7%)	0.61	1.00	3/12 (25%)	.19	.67
IRF8	13/37 (35.1%)	8/22 (36.4%)	1.00	1.00	4/13 (30.8%)	1.00	1.00
IRF8 (p.K66R)	12/37 (32.4%)	5/22 (22.7%)	.57	1.00	2/13 (15.4%)	.30	.67
IRF8 (p.Y23H)	2/37 (5.4%)	4/22 (18.2%)	.18	.92	1/13 (7.7%)	1.00	1.00
EZH2	0/38	0/20	1.00	1.00	2/11 (18.2%)	**.05**	.35
FOXO1	1/38 (2.6%)	1/20 (5%)	1.00	1.00	0/11	1.00	1.00
GNA13	4/38 (10.5%)	1/20 (5%)	.65	1.00	0/11	.56	1.00
HIST1H1D	0/38	0/20	1.00	1.00	1/11 (9.1%)	.22	.67
HIST1H1C	1/38 (2.6%)	1/20 (5%)	1.00	1.00	0/11	1.00	1.00
KMT2D	6/38 (15.8%)	0/24	.07	.55	0/12	.31	.79
HIST1H1B	1/38 (2.6%)	0/20	1.00	1.00	0/11	1.00	1.00
EP300	2/38 (5.3%)	0/20	.54	1.00	0/11	1.00	1.00
CREBBP	1/38 (2.6%)	0/20	1.00	1.00	0/11	1.00	1.00
TNFRSF14 biallelic inactivation	15/39 (38.5%)	3/23 (13%)	**.04**	.55	0/12	**.01**	.16

Statistically significant *P* values are highlighted in bold.

could be the inherent differences in the 2 methods used. Nevertheless, recurrent trisomy 18 is infrequently identified in PNMZL. The mutational profile of PNMZL was also found to be distinct from adult-type NMZL, with *MAP2K1* mutations found exclusively in the pediatric group, and mutations affecting genes (including *KMT2D*, *KLF2, TBL1XR1, NOTCH2*, and *TNFAIP3*) that are frequently found in adult-type NMZL[5] were absent in PNMZL. Nevertheless, the diagnosis of PNMZL should be considered in the differential diagnosis of limited-stage NMZL.

Prior studies have noted clinical similarities between PTFL and PNMZL.[21,22] One of the interesting observations in our large series was the extent of morphologic overlap between PNMZL and PTFL, with many cases that were originally diagnosed as PNMZL showing some degree of histologic overlap with PTFL upon review. This, together with the original 13 cases diagnosed as having overlapping features, indicates that the majority of the cases diagnosed as PNMZL have morphologic overlap with PTFL (31 of 45 cases [69%]). A notable architectural feature of overlap in these cases was the presence of at least some follicles with attenuated mantle zones and large germinal centers strongly positive for CD10 characteristic of PTFL and indicative of a subpopulation with germinal center cell phenotype. Accordingly, the morphologic overlap between them has been previously noted, and cases of PTFL with marginal zone differentiation[2-4] or cases of PNMZL harboring CD10 positivity and light chain–restricted populations by flow cytometry[22] have been described. In this study, mutations in *MAP2K1, TNFRSF14,* and *IRF8* were more frequently observed in cases with morphologic overlap with PTFL (n = 22 of 28 [78%]), compared with those cases without (n = 8 of 13 [61%]); however, this difference was not statistically significant. Nevertheless, the high percentage of PNMZL cases carrying 1 or more of these 3 mutations in the whole collective (73%) suggests that PTFL and PNMZL form part of a histologic continuum and, given the genetic similarities, could represent a morphologic spectrum within the same biologic entity. One could speculate that because of the different effects of *MAP2K1*, *TNFRSF14*, and *IRF8* in the maturation of B cells, the genetic constellation in each case might imprint the observed morphology (with or without marginal zone differentiation), immunophenotype, and maturation stage.[11]

Given the morphologic similarities of PNMZL to a reactive process, we analyzed 5 cases of reactive lymph nodes, mainly atypical marginal zone hyperplasia, and confirmed that this is a benign process that lacks the monoclonal IG rearrangements and genetic alterations that are diagnostic of PNMZL. However, our study also highlighted the difficulty in separating atypical marginal zone hyperplasia from PNMZL in routine practice, underscoring that the diagnosis of PNMZL still rests on the combination of morphology and demonstration of B-cell clonality.

In conclusion, this study shows that PNMZL is a neoplastic condition that is distinct from atypical marginal zone hyperplasia and adult-type NMZL but displays overlapping histologic and molecular features with PTFL, suggesting that PNMZL and PTFL may represent a morphologic spectrum within the same biologic entity. Due to the indolent clinical behavior and similar morphologic and genetic features, we suggest renaming these entities under the name of "pediatric-type follicular lymphoma (PTFL) with and without marginal zone differentiation."

Acknowledgments

The authors thank the centers of the Sociedad Española de Hematología y Oncología Pediátricas-SEHOP that submitted cases for consultation and Noelia Garcia, Silvia Martín, and Helena Suarez for their excellent technical assistance. They are indebted to the IDIBAPS Genomics Core Facility and to HCB-IDIBAPS Biobank–Tumor Bank and Biobanc de l'Hospital Infantil Sant Joan de Déu for sample and data procurement.

This work was supported by Asociación Española Contra el Cáncer (AECC CICPFI6025SALA), Fondo de Investigaciones Sanitarias Instituto de Salud Carlos III (Miguel Servet Program CP13/

00159 and CPII18/00015, I.S.), Generalitat de Catalunya Suport Grups de Recerca (2017-SGR-1107, I.S.; 2017-SGR-1142, E.C.) and Acció instrumental d'incorporació de científics i tecnòlegs PERIS 2016 (SLT002/16/00336), and the European Regional Development Fund "Una manera de fer Europa." J.S.-V. was supported by a fellowship from La Caixa (CLLEvolution-HR17-00221). The work of R.S. and S.G. on DNA methylation of lymphomas was performed in the framework of the Deutsche Forschungsgemeinschaft (German Research foundation) funded SFB 1074 (project B9). E.C. is an Academia Researcher of the "Institució Catalana de Recerca i Estudis Avançats" (ICREA) of the Generalitat de Catalunya. This work was partially developed at the Centro Esther Koplowitz, Barcelona, Spain. E.S.J. is supported by the Intramural Research Program of the Center for Cancer Research, National Cancer Institute, National Institutes of Health (ZIA SC 000550). L.Q.-M. is funded by the Deutsche Forschungsgemeinschaft (German Research foundation) under Germany's Excellence Strategy, EXC2180-390900677.

Authorship

Contribution: J.S.-V., C.E., and V.B. performed research, analyzed data, and wrote the manuscript; B.G.-F. performed morphologic diagnosis and analyzed data; J.E.R.-Z., I.B., D.N., S.G., and R.S. performed research and analyzed data; O.B., W.K., I.O., Y.H.K., and S.P. contributed with cases and performed pathologic reviews; M.L.-G., I.M., and D.C. performed molecular analyses; F.F. and E.C. performed morphologic analysis, designed research, and helped write the paper; I.S., L.Q.-M., and E.S.J. performed research, analyzed data, designed research, and wrote the manuscript; and all authors approved the final manuscript.

Conflict-of-interest disclosure: The authors declare no competing financial interests.

ORCID profiles: J.S.-V., 0000-0002-7092-9160; B.G.-F., 0000-0002-1796-7248; J.E.R-Z., 0000-0001-7108-7738; D.N., 0000-0002-3071-793X; O.B., 0000-0002-5099-3675; M.L.-G., 0000-0002-5545-0178; D.C., 0000-0001-7486-8484; W.K., 0000-0001-7208-4117; Y.H.K., 0000-0002-4383-0579; I.B., 0000-0002-7732-0788; F.F., 0000-0002-5496-293X; S.P., 0000-0001-7688-1439; E.C., 0000-0001-9850-9793; I.S., 0000-0002-2427-9822; E.S.J., 0000-0003-4632-0301; L.Q.-M., 0000-0001-7156-5365.

Correspondence: Elaine S. Jaffe, Hematopathology Section, Laboratory of Pathology, Center for Cancer Research, National Cancer Institute, National Institutes of Health, Building 10/Room 3S 235, 10 Center Dr, MSC-1500, Bethesda, MD 20892-1500; e-mail: ejaffe@mail.nih.gov; Leticia Quintanilla-Martinez, Institute of Pathology, University Hospital Tübingen, Liebermeisterstrasse 8, 72076 Tübingen, Germany; e-mail: leticia.quintanilla-fend@med.uni-tuebingen.de; and Itziar Salaverria, Institut d'Investigacions Biomèdiques August Pi i Sunyer (IDIBAPS), Rosselló 153, 08036 Barcelona, Spain, e-mail: isalaver@recerca.clinic.cat.

References

1. Taddesse-Heath L, Pittaluga S, Sorbara L, Bussey M, Raffeld M, Jaffe ES. Marginal zone B-cell lymphoma in children and young adults. *Am J Surg Pathol.* 2003;27(4):522-531.
2. Liu Q, Salaverria I, Pittaluga S, et al. Follicular lymphomas in children and young adults: a comparison of the pediatric variant with usual follicular lymphoma. *Am J Surg Pathol.* 2013;37(3):333-343.
3. Louissaint A Jr, Ackerman AM, Dias-Santagata D, et al. Pediatric-type nodal follicular lymphoma: an indolent clonal proliferation in children and adults with high proliferation index and no BCL2 rearrangement. *Blood.* 2012;120(12):2395-2404.
4. Wong JT, Armenian S, Nathwani BN. A pediatric-type follicular lymphoma with marginal zone and monotypic intracytoplasmic plasmacytic differentiation. *Hum Pathol Case Reports.* 2018;11:25-31.
5. Spina V, Khiabanian H, Messina M, et al. The genetics of nodal marginal zone lymphoma. *Blood.* 2016;128(10):1362-1373.
6. Pillonel V, Juskevicius D, Ng CKY, et al. High-throughput sequencing of nodal marginal zone lymphomas identifies recurrent BRAF mutations. *Leukemia.* 2018;32(11):2412-2426.
7. Schmidt J, Gong S, Marafioti T, et al. Genome-wide analysis of pediatric-type follicular lymphoma reveals low genetic complexity and recurrent alterations of TNFRSF14 gene. *Blood.* 2016;128(8):1101-1111.
8. Schmidt J, Ramis-Zaldivar JE, Nadeu F, et al. Mutations of *MAP2K1* are frequent in pediatric-type follicular lymphoma and result in ERK pathway activation. *Blood.* 2017;130(3):323-327.
9. Louissaint A Jr, Schafernak KT, Geyer JT, et al. Pediatric-type nodal follicular lymphoma: a biologically distinct lymphoma with frequent MAPK pathway mutations. *Blood.* 2016;128(8):1093-1100.
10. Martin-Guerrero I, Salaverria I, Burkhardt B, et al. Recurrent loss of heterozygosity in 1p36 associated with TNFRSF14 mutations in IRF4 translocation negative pediatric follicular lymphomas. *Haematologica.* 2013;98(8):1237-1241.
11. Ozawa MG, Bhaduri A, Chisholm KM, et al. A study of the mutational landscape of pediatric-type follicular lymphoma and pediatric nodal marginal zone lymphoma. *Mod Pathol.* 2016;29(10):1212-1220.
12. Rizzo KA, Streubel B, Pittaluga S, et al. Marginal zone lymphomas in children and the young adult population; characterization of genetic aberrations by FISH and RT-PCR. *Mod Pathol.* 2010;23(6):866-873.
13. Swerdlow SH, Campo E, Harris NL, et al,.eds. WHO Classification of Tumours of Haematopoietic and Lymphoid Tissues (Revised 4th edition). Lyon, France: IARC 2017.

14. van Dongen JJ, Langerak AW, Brüggemann M, et al. Design and standardization of PCR primers and protocols for detection of clonal immunoglobulin and T-cell receptor gene recombinations in suspect lymphoproliferations: report of the BIOMED-2 Concerted Action BMH4-CT98-3936. *Leukemia.* 2003;17(12):2257-2317.

15. Nadeu F, Royo R, Maura F, et al. Minimal spatial heterogeneity in chronic lymphocytic leukemia at diagnosis. *Leukemia.* 2020;34(7):1929-1933.

16. Kridel R, Sehn LH, Gascoyne RD. Pathogenesis of follicular lymphoma. *J Clin Invest.* 2012;122(10):3424-3431.

17. Okosun J, Bödör C, Wang J, et al. Integrated genomic analysis identifies recurrent mutations and evolution patterns driving the initiation and progression of follicular lymphoma. *Nat Genet.* 2014;46(2):176-181.

18. Karube K, Martínez D, Royo C, et al. Recurrent mutations of NOTCH genes in follicular lymphoma identify a distinctive subset of tumours. *J Pathol.* 2014;234(3):423-430.

19. Vogt J, Wagener R, Montesinos-Rongen M, et al. Array-based profiling of the lymphoma cell DNA methylome does not unequivocally distinguish primary lymphomas of the central nervous system from non-CNS diffuse large B-cell lymphomas. *Genes Chromosomes Cancer.* 2019;58(1):66-69.

20. Karube K, Enjuanes A, Dlouhy I, et al. Integrating genomic alterations in diffuse large B-cell lymphoma identifies new relevant pathways and potential therapeutic targets. *Leukemia.* 2018;32(3):675-684.

21. Ganapathi KA, Pittaluga S, Odejide OO, Freedman AS, Jaffe ES. Early lymphoid lesions: conceptual, diagnostic and clinical challenges. *Haematologica.* 2014;99(9):1421-1432.

22. Quintanilla-Martinez L, Sander B, Chan JKC, et al. Indolent lymphomas in the pediatric population: follicular lymphoma, IRF4/MUM1+ lymphoma, nodal marginal zone lymphoma and chronic lymphocytic leukemia. *Virchows Arch.* 2016;468(2):141-157.

23. Šedý JR, Ramezani-Rad P. HVEM network signaling in cancer. *Adv Cancer Res.* 2019;142:145-186.

24. Boice M, Salloum D, Mourcin F, et al. Loss of the HVEM tumor suppressor in lymphoma and restoration by modified CAR-T cells. *Cell.* 2016; 167(2):405-418.e13.

25. Lu R. Interferon regulatory factor 4 and 8 in B-cell development. *Trends Immunol.* 2008;29(10):487-492.